2010 IEEE International Conference on Robotics and Automation
Anchorage Convention District
May 3-8, 2010, Anchorage, Alaska, USA

Development of a Low Motion-Noise Humanoid Neck: Statics Analysis and Experimental Validation

Bingtuan Gao, Ning Xi, Yantao Shen, Jianguo Zhao and Ruiguo Yang

Abstract— **This paper presents our recently developed humanoid neck system that can effectively mimic motion of human neck with very low motion noises. The feature of low motion noises allows our system to work like a real human head/neck. Thus the level of acoustic noises from wearable equipments, such as donning respirators or chemical-resistant jackets, induced by human head motion can be simulated and investigated using such a system. The objective of this investigation is to facilitate using head-worn communication devices for the person who wears the protective equipment/uniform that usually produces communication-noise when the head/neck moves.**

Our low motion-noise humanoid neck system is based on the spring structure, which can generate 1 Degree of Freedom (DOF) jaw movement and 3DOF neck movement. To guarantee the low-noise feature, no noise-makers like gear and electro-driven parts are embedded in the head/neck structure. Instead, the motions are driven by seven cables, and the actuators pulling the cables are sealed in a sound insulation box. Furthermore, statics analysis of the system has been processed completely. Experimental results validate the analysis, and clearly show that the head/neck system can greatly mimic the motions of human head with an A-weighted noise level of 30 dB or below.

I. INTRODUCTION

Human head motion relies on the flexibility and strength of neck muscles and back-bone. Human neck attaches the head to the trunk and facilitates its movements. The complex kinematics of the human neck is defined by the cervical portion of the human spine which contains seven cervical vertebrae, typically referred as C1 to C7. Among these vertebrae, the first vertebrae, called the atlas vertebra (C1), supports head. The second vertebrae, called the axis vertebra (C2), pivots to turn head. The joints between these two vertebrae give the neck most of its rotation [1]. Although each vertebra has 6DOF , researchers take the overall neck as 6DOF, corresponding to 3DOF rotation and 3DOF translation. From practical point of view, the translation effects are neglected in most applications; as a result, human neck is simplified as a structure with only 3DOF: buckling of the head forward (flex) and backward (extend), buckling, and rotating the head to the left and right, or can be called pitch, roll, and yaw, respectively.

This work is partially supported by US ARMY Research under the contract of W911SR-08-C-0027.

Bingtuan Gao, Ning Xi, Jianguo Zhao, and Ruiguo Yang are with Department of Electrical and Computer Engineering, Michigan State University, East Lansing, MI 48824, USA. gaopu1089@gmail.com, xin@egr.msu.edu, zhaojia1@msu.edu, yangruig@msu.edu

Yantao Shen is with Department of Electrical and Biomedical Engineering, University of Nevada at Reno, Reno, NV 89557-0260, USA. ytshen@unr.edu

A. Literature Review

Numerous human-like robots or humanoid robots were developed and have been becoming our partners in our daily life. Different humanoid robots have different functions. For instance, Sony Qrio [2] which has totally 38 DOF was designed to interact with people; Honda ASIMO [3] which is driven by 26 DOF can entertain and serve people; Hiroshi [4] designed an android with his appearance that can be teleoperated instead of the presence himself; iCub [5] was designed to study cognition through the implementation of a humanoid robot the size of a two years old child; etc. For all developed or developing this class of humanoid robots, an appropriate robotic neck has to be necessarily considered.

Although there are many humanoid neck mechanisms developed by different institutions, they can be divided into four categories, i.e. serial neck, parallel neck, spring-based neck, and spherical neck. Among the mechanisms, serial necks are the most common mechanisms due to simple structure and easiness of DC motor control. The HRP-2 [6] has a 2 DOF serial neck including pitch and yaw. The Albert HUBO [7], the Dav [8], and the iCub [5] have 3 DOF serial necks. The WE-4 [9], the ARMAR-III [10], the WABIAN-RIV [11], and the ROMAN [12] have 4 DOF serial necks. Parallel neck just likes a Stewart Platform [5], which needs a passive spine and is controlled by several legs with combination of universal, prismatic, and spherical joints. The actuators for the parallel necks can be DC motors or pneumatic cylinders. Parallel mechanisms have the characteristics of rigidity, high load capacity, and high precision; however, it is hard to reach large motion range and not suitable to be used in the limited neck space. Spherical neck means the motion of the neck is basically based on a spherical joint. Using the screw theory, Sabater et al. [13] designed and analyzed a spherical humanoid neck. The entertainment robot WoWWee Alive Elvis [14] also has a spherical neck. Spring neck is the mechanism that uses a spring as the spine to support head and facilitate its motion. Spring neck can usually be driven by motors [5] and artificial muscles [15]. According to previous investigation, spring neck is in good similarity to the real human neck and it is economical to build; however, it is hard to achieve high precision positioning control because of the complicated dynamics of the springs.

Most of the research on humanoid robotic necks do provide much insight into how to make the neck move like that of human beings. However, little research adequately addresses how to design a robotic neck that can move quietly like the neck of human beings.

B. Motivation and Contributions

People need to wear donning respirators or chemical-resistant jackets in some emergent conditions or during performing some special tasks. Most of current donning respirators or chemical-resistant jackets generate the acoustic noises unavoidably when users move their heads/necks. These noises strongly interfere users' hearing even users take head-worn wireless communication equipments. This disturbance could hinder the communication significantly or even cause user lose their lives when they mishear commands during some dangerous tasks. Thus, it becomes necessary to investigate the acoustic issues associated with above mentioned cases. Under this requirement, a special humanoid robotic head/neck system is developed. The size of the developed head/neck is the same as average human beings. More importantly, it can mimic human head/neck in both motion and the biological performance like low motion-noise. The main challenges of this development is in the design and control of such a low motion-noise biomimetic 3DOF head/neck system. The system will be used for investigating the level of acoustic noises produced by the interactive motion between wearable equipments and human head/neck, so as to facilitate using head-worn communication devices.

Inspired by human neck structure, the main part of the developed head/neck is a compressed column spring that has the similar function as that of the back-bone. It supports the artificial/robotic head, and can buckle around the neutral axis to generate 2DOF rotation including pitch and roll motions. A cable-pulley structure that is mounted above the spring is used to realize the remained yaw motion. The 3DOF motion of the neck is realized through driving six cables that have similar functions of human neck muscles. These cables are pulled by the actuators sealed in a sound insulation box. As no sound generation parts are embedded into the robotic neck, there are only very low motion noises generated by the neck during its motions.

Main contributions of this paper are as follows:

- Description and comparison on development of a spring-based humanoid head/neck system with low motion-noise.
- Analysis on lateral buckling of the spring-based robotic neck with elasticity theory by considering the spring as a prismatic bar while considering the change in length of the spring.

II. LOW MOTION-NOISE HUMANOID HEAD/NECK SYSTEM

A. System Overview

The picture of the developed robotic system is shown in Fig. 1. The system consists of a humanoid robotic unit, a cable-and-housing group, a sound insulation box, and a personal computer (PC). The robotic unit has a movable robotic head, a torso, and a height adjustable support frame used to match human with different height or either sitting or standing status. The size of the head and torso is designed following the head size of a human adult so that full size

Fig. 1. A picture of the low motion-noise humanoid head/neck system

personal protective uniform can fit the robotic system very well. The movable robotic head includes a 1DOF jaw motion part to mimic human mouth motion when speaking and a 3DOF neck framework to mimic human neck's movement. These movements are driven by the remote motor-based actuators installed in the sound insulation box through the compound cable-and-housing group. The motor-based actuators are controlled by a PC via a PCI-based motion controller board, and the control/driven strategy of the motor system is developed and conducted using the PC.

In the system, cable housings are used to guide the driving cables or to transmit the outputs of actuators from the sound insulation box to the robot head. It would be a novel design if use cable housings to guide the driving cables in cable-driven mechanisms. We found at least three advantages for utilizing cable-and-housing group in this system:

1) simplifying the mechanical transmission design significantly;
2) generating few noises by the cable-and-housing group,
3) facilitating the sealing issue for the sound insulation box.

The materials of the driving cables are the braided polyester. The used housings are typical bicycle brake cable housings. As there is one layer of lubricated inner in the cable housing, the friction coefficient is relatively low between the cable and its housing. It should be noted that the steel driving cables can transmit noises out from the sound insulation box, in which motors, gearboxes and corresponding electrical parts are installed, to the robotic head/neck.

B. Hardware Development

Major hardware components in the system are the robotic neck and the sound insulation box.

Robotic neck: The CAD assembly model of the 3DOF robotic neck is shown in Fig. 2. A compressive spring connecting two plates serves as the main mechanical structure of the robotic neck. The plate 2 is fixed to the torso while the plate 1 together with all parts mounted on it can be buckled by the four symmetrically distributed driving cables, thus

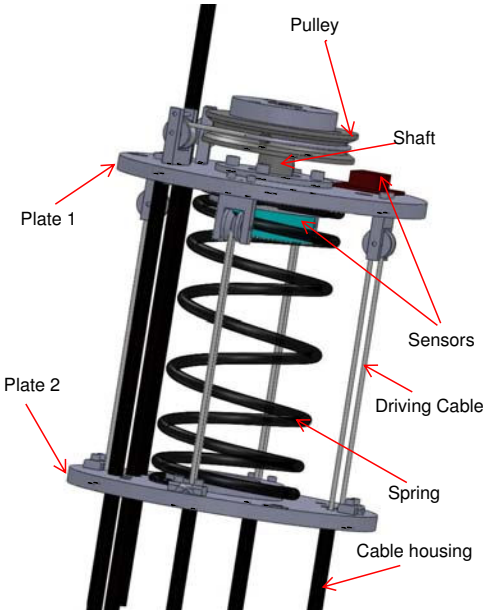

Fig. 2. CAD assembly model of 3DOF robotic neck

the plate 1 can realize 2DOF rotation including pitch and roll (the single axis motions correspond the head motions flexion, extension, bending left, and bending right). The four small pulleys mounted on the bottom surface of the plate 1 are used to enhance the buckling force exerted by the cables. The one end of each driving cable is fixed on the plate 2. These four cables are guided to the robotic neck by their cable housings, and the one end of each cable housing is fixed into the plate 2.

The yaw motion of the robotic head, mimicking human head's yaw motion, can be achieved by using a cable-and-pulley structure which is connected to the plate 1 via a shaft and ball bearing group. As a result, the yaw motion of the robotic head is designed to be realized by the structure locating on the top of the robotic neck. This design is coincidence with the fact that most of the yaw motion of human head is generated between the C1 and C2 cervical vertebrae. The shaft and ball bearing group in the structure can effectively reduce the friction and motion noises of the rolling shaft during the yaw motion. As the cable housings used to guide the yaw driving cables can not be mounted well with a small curvature radius within the small space, they are fixed at the plate 1. Instead, two small pulleys are used to guide the two cables to realize yaw motion.

The robotic head including the jaw motion structure is assembled onto the neck structure through the head mounting piece together with the yaw pulley, as shown in Fig. 2. The cable-and-housing stretched over the pulley will be used to drive the jaw motion.

In addition, two sensors for monitoring the motion of the 3DOF neck are mounted, as shown in Fig. 2. One is a 2-axis inclinometer that measures the pitch and roll angles, which is mounted on the top surface of the plate 1. The other is a potentiometer for measuring the yaw motion angle. The shaft of the potentiometer is fixed with the yaw pulley through the shaft and bearing group.

Sound insulation box: There are two natural ways to remove the noises passively. One is sound insulation and the other is sound absorption. Sound insulation is to eliminate the sound path from a source. Usually the high-density materials are the best choices for sound insulation. Sound absorption works when some or all of the incident sound energy are either converted into heat or pass through the absorbers like porous foams. To greatly prevent the sound transmission from the box, sound insulation and sound absorption techniques are both adopted. The box itself is made by heavy material 12-gauge cold rolled steel with the sound leakproof method. The six inner walls of the box are covered by 10mm thick butyl rubber that has good acoustic absorption effects. The rubber helps to absorb the noises with the frequencies between 30Hz and 4000Hz.

In summary, since (1) no noiseful gear and electro-driven parts are embedded in the bio-mimetic head/neck structure, (2) sound generation parts are sealed in the sound insulation box, and (3) the driving system are dominated by the low-friction and high efficient cable-and-housing group, the developed humanoid head/neck system could greatly mimic the motion of human head without generating unacceptable motion noises.

C. *Functionalized Head Movements*

Reference to the motions of human head/neck and mouth, the 3DOF neck motion and 1DOF jaw motion can fulfill seven single movements including head flexion, head extension, bending head left, bending head right, rotating head left, rotating head right, and opening mouth. The instruction for each movement has two programmable parameters: movement range and movement time. In other words, the position and velocity of each movement can be defined. All non-conflicting multi-axis combined movements and a sequence of movements are allowed to perform with the developed robotic system. This means all complex movements associated with human neck can be conducted by the robotic head/neck.

III. LATERAL BUCKLING OF THE ROBOTIC NECK

The pitch and roll motion mechanism of the humanoid neck is a practical lateral buckling problem of compressed helical springs. The classic treatise on the behavior of helical spring could be found in Wittrick's paper [16]. Wittrick treated the helical spring as a Timoshenko beam including shear deformation and rotational inertia and derived a set of 12 linear coupled partial differential equations which have been used by a number of authors. Timoshenko [17] investigated the rigidity of the compression, lateral and shear deflections for a coil spring to explain the bounds of stability of a compressed helical spring due to buckling. The same results were also concluded by Wahl [18] in 1963. Timoshenko [17] also pointed out that lateral buckling of coil compressed spring can be studied by the same methods as

the prismatic bars but it is necessary to consider the change in length of the spring due to compression, since the change is not negligible in the case of compressed bars.

Now we assume the notations of the selected helical spring as following: l_0 is the initial length of the spring; h_0 is the pitch of the helix; n is the number of coils; r is the radius of the helix; l is the length of the spring after compression; I is the moment of inertia of the cross section of the wire with respect to its diameter; α_0, β_0, γ_0 are the compressive, flexural and shearing rigidities of the helical spring and they take the place of the quantities AE, EI and AG/n for the case of solid bar; α, β, γ are the same quantities after compression of the spring. It is shown that these quantities are inversely proportional to the number of coils per unit length of the spring [17], hence,

$$\alpha = \alpha_0 \frac{l}{l_0}, \tag{1}$$

$$\beta = \beta_0 \frac{l}{l_0}, \tag{2}$$

$$\gamma = \gamma_0 \frac{l}{l_0}. \tag{3}$$

where the compressive, flexural and shearing rigidities can be calculated as

$$\alpha_0 = \frac{GIl_0}{\pi n r^3}, \tag{4}$$

$$\beta_0 = \frac{2EGIh_0}{\pi r(E+2G)}, \tag{5}$$

$$\gamma_0 = \frac{EIh_0}{\pi r^3}. \tag{6}$$

The general lateral buckling of the spring-based mechanism can be depicted in Fig. 3. The total mass of the upper plate is taken as a point mass at the mobile plate's center with quantity m_0. The payload at (r_y, α_y) with quantity m_e is attached to the mobile plate's center. The spring-based mechanism is driven by two cables with the applied force T_1 and T_3 through the plate 1 at the points a measured away from its center. And the locations of the cables passing through the plate 2 are b from the center. By taking the coordinate axes as indicated in Fig. 3, the buckling moment at any cross section of the spring is M and its deflection curve becomes:

$$\beta \frac{\frac{d^2y}{dz^2}}{(1+(\frac{dy}{dz})^2)^{\frac{3}{2}}} = M. \tag{7}$$

The total moment M applied to buckle the spring consists of four parts: the torque generated by the mass of mobile plate 1 itself M_{m_0}, the torque generated by the external payload M_{m_e}, the torque generated by the cable forces M_{T_1} and M_{T_3}. Thus we have

$$\begin{aligned} M &= M_{m_0} + M_{m_y} + M_{T_1} + M_{T_3} \\ &= (m_0 g + m_e g + T_1 \cos\alpha_1 + T_3 \cos\alpha_3)(y_b - y) \\ &\quad -(T_1 \sin\alpha_1 + T_3 \sin\alpha_3)(l - z) + m_e g r_y \cos\alpha_y \\ &\quad +T_1 \cos\alpha_1 a \cos\theta_x + T_1 \sin\alpha_1 a \sin\theta_x \\ &\quad -T_3 \cos\alpha_3 a \cos\theta_x - T_3 \sin\alpha_3 a \sin\theta_x. \end{aligned} \tag{8}$$

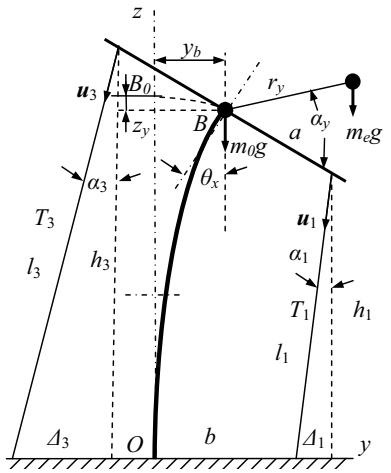

Fig. 3. Lateral buckling model of the spring-based mechanism

Equation (7) does not have an analytical solution but it can be obtained by calculating elliptic integrals [19], which can be evaluated using numerical methods. For small deflection, equation (7) can be rewritten as a linear case:

$$\beta \frac{d^2y}{dz^2} = M. \tag{9}$$

Although an adult human heads can buckle more than 40deg in one direction for pitch and roll motions respectively, the motion of our head are usually no more than 15deg buckled in all three axes in our daily life [21]. Thus, it is feasible to use the linear equation (9) to calculate statics model of lateral buckling for the cable-driven robotic head/neck in this application.

By considering the initial conditions

$$(y)_{z=0} = 0, \left(\frac{dy}{dz}\right)_{z=0} = 0,$$

the general solution of (9) is obtained as:

$$y = (y_b + a_0)(1 - \cos wz) - \frac{a_1}{w}\sin wz + a_1 z, \tag{10}$$

where

$$w = \sqrt{\frac{m_0 g + m_y g + T_1 \cos\alpha_1 + T_3 \cos\alpha_3}{\beta}}, \tag{11}$$

$$\begin{aligned} a_0 &= [m_e g r_y \cos\alpha_y + T_1 \cos\alpha_1 a \cos\theta_x \\ &\quad +T_1 \sin\alpha_1 a \sin\theta_x - T_3 \cos\alpha_3 a \cos\theta_x \\ &\quad -T_3 \sin\alpha_3 a \sin\theta_x - (T_1 \sin\alpha_1 + T_3 \sin\alpha_3) l] \\ &\quad (m_0 g + m_e g + T_1 \cos\alpha_1 + T_3 \cos\alpha_3)^{-1}, \end{aligned} \tag{12}$$

$$\begin{aligned} a_1 &= (T_1 \sin\alpha_1 + T_3 \sin\alpha_3) \\ &\quad (m_0 g + m_e g + T_1 \cos\alpha_1 + T_3 \cos\alpha_3)^{-1}. \end{aligned} \tag{13}$$

The condition at the top end of the spring requires

$$y_b = (y)_{z=l} = (y_b + a_0)(1 - \cos wl) - \frac{a_1}{w}\sin wl + a_1 l,$$

so that

$$y_b = \frac{1 - \cos wl}{\cos wl} a_0 - \frac{a_1}{w}\tan wl + \frac{a_1 l}{\cos wl}. \tag{14}$$

Then the statics buckling model (10) can be rewritten as

$$y = (\frac{1}{\cos wl}a_0 - \frac{a_1}{w}\tan wl + \frac{a_1 l}{\cos wl})(1-\cos wz) - \frac{a_1}{w}\sin wz + a_1 z.$$

Also, the deflection angle at the top end of the spring gives

$$\theta_x \approx y'_{z=l} = a_0 w \tan wl + a_1(1 - \sec wl + wl \tan wl). \quad (15)$$

The corresponding vertical displacement of the spring under buckling from B_0 to B, as shown in Fig. 3, can be calculated with [20]

$$\begin{aligned} z_y &\approx \frac{1}{2}\int_0^l \left(\frac{dy}{dz}\right)^2 dz \quad (16)\\ &= \frac{1}{2}\int_0^l ((y_b + a_0)w\sin wz - a_1\cos wz + a_1)^2\, dz \\ &= \frac{\sec^2(wl)}{8w}\{-4a_0a_1w + 8a_1(a_0+a_1l)w\cos(wl) \\ &\quad +2(a_0+a_1l)^2w^3l - 4a_1l(a_0+a_1l)w^2\sin(wl) \\ &\quad -2a_1(2a_0+a_1l)w\cos(2wl) \\ &\quad -[3a_1^2 + (a_0+a_1l)^2w^2]\sin(2wl)\}. \end{aligned}$$

For the cable length calculation, according to illustration in Fig. 3, we have

$$\alpha_1 = \arctan\frac{\Delta_1}{h_1}, \quad (17)$$

$$l_1 = \sqrt{\Delta_1^2 + h_1^2}, \quad (18)$$

$$\alpha_3 = \arctan\frac{\Delta_3}{h_3}, \quad (19)$$

$$l_3 = \sqrt{\Delta_3^2 + h_3^2}, \quad (20)$$

where

$$\begin{aligned} \Delta_1 &= y_b + a\cos\theta_x - b, \\ h_1 &= l - z_y - a\sin\theta_x, \\ \Delta_3 &= b - (a\cos\theta_x - y_b), \\ h_3 &= h_1 + 2a\sin\theta_x. \end{aligned}$$

The spring length l under compression is calculated as

$$l = l_0 - \Delta l, \quad (21)$$

where

$$\Delta l = \frac{1}{K}[m_0 g + m_e g + \sum_{i=1}^{2} T_i \cos\alpha_i]$$

and K is the spring stiffness.

Based on the general planar buckling configuration shown in Fig. 3, for given moving mechanism of the robot neck and its payloads, the parameters of l_0, K, a, b, m_0, m_e, and (r_y, α_y) are known constants. We have eight independent equations (14-21) in buckling angle θ_x, compressed spring length l, cable length l_1 and its direction α_1, cable length l_3 and its direction α_3, vertical displacement of the spring under buckling z_y, and horizontal displacement of the spring under buckling y_b. For the case of finding out buckling angle θ_x for given cable force T_1 and T_3, all unknown parameters can be solved using the equations. However, it is a redundant problem to find out T_1 and T_3 for given buckling angle θ_x. Here, we employ an effective simple solution. Only one of the two driving cables is used to buckle the mechanism by evaluating the buckling angle θ_x, mass m_0, and payload m_e at (r_y, α_y). In other words, one of the driving cable force T_1 and T_3 will be set to zero. For example, as depicted in Fig. 3, once no payload is applied, we only employ T_1 to buckle the mechanism as the mass m_0 is not large enough to buckle the spring. Consequently, all other unknown parameters can be determined.

TABLE I

PARAMETERS OF SELECTED COMPRESSIVE SPRING

l_0(m)	h_0(m)	n	G(MPa)	E(MPa)	r(m)	d(m)
0.1016	0.0195	5.2	77,200	196, 500	0.0227	0.0038
Material: Spring-Tempered Steel						

IV. EXPERIMENTAL VALIDATION

A. Lateral Buckling Test

Physical parameters of selected compressive column spring for the spring-based robotic neck are shown in Table I. Using these parameters, we can get the following items of the spring: $I = \pi d^4/64 = 1.023 \times 10^{-11}\text{m}^4$, $K = Gd^4/64nr^3 = 4.151 \times 10^3\text{N/m}$, and $\beta_0 = 0.2420$.

In order to verify the statics model, an experiment was implemented. The spring used has the same parameters shown in Table I and additional parameters includes $m_0 = 0.093$kg, $a = b = 0.061$m, $m_e = T_3 = 0$. A force sensor from Futek advanced tech. with measure range 0 to 44.5N and a dual axis angle sensor from VTI Tech. with measure range 0 to 90° were used in the experiment. Experimental results were shown in Fig. 4. The curve with experimental data showed that the angle of the buckling was apparently proportional to the force input. The fitting linear curve was $\theta_x = 1.6312T_1 + 2.0712$, as shown in the figure. Although the line should pass through the origin theoretically, the practical installation of the setup can't be absolutely horizontal. This results the zero-offset in the plot. In the figure, we also presented the curve of (15) with the practical force data. The result shows that the experimental angle and calculation angle based on (15) have good agreement. This indicates that the developed statics model of lateral buckling for the spring-based mechanism was effective under small buckling angle.

B. Motion Noise Test

Single and combination head motions have been implemented successfully on the developed low motion-noise robotic head/neck system. The instructed robotic head movements, which are demonstrated in Fig. 5, are: 30deg flexion, 45deg extension, 30deg bending left, 30deg bending right, 60deg rotating left, 60deg rotating right, and 20mm opening mouth.

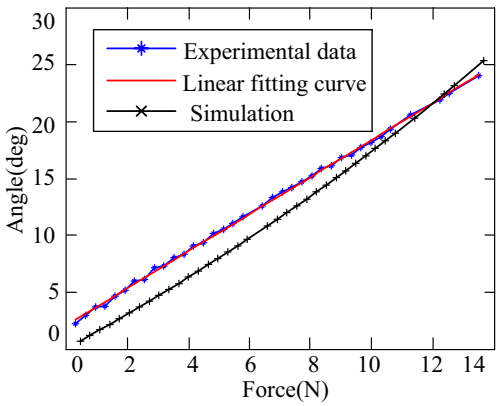

Fig. 4. Experiment results with simulation comparison

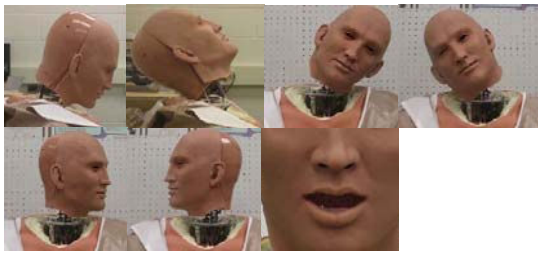

Fig. 5. Pictures of the instructed seven single movements

An anechoic chamber at Michigan State University was used as an acoustic room to test the noise level of the robotic head/neck system during its motion. The noise level of the system during its motions was monitored by a sound level alert from Extech Instruments. The experimental result showed that the maximum noise level of the system during different motions was no more than 30dB A weighted, which was in quite low motion noise level that meets the requirement of the further acoustic research projects.

V. CONCLUSIONS

We present a spring-based cable-driven humanoid head/neck system which can produce 3DOF neck motions and 1DOF jaw motion with very low motion-noise level in this paper. Three main ideas are fulfilled to reduce the noises as follows: 1) using a compressive helical spring to mimic cervical vertebrae and using cables to mimic muscles, which guarantee no major noise-makers such as gear and electro-driven parts are embedded in the head/neck structure, 2) remotely driving the head/neck system using the cable-and-housing group, which guarantees low-friction and low noise transmission, 3) the noiseful cable-pulling actuators are sealed in a sound insulation box. To validate the design of the system, both theoretical statics analysis and experiments are implemented. The experimental results clearly show the system performance has good agreement with the theoretical analysis, and also prove the effectiveness of the designed head/neck system. The system can be effectively used to investigate the level of acoustic noises produced by the interactive motion between wearable equipments/uniforms and human head/neck, so as to facilitate using head-worn communication devices.

VI. ACKNOWLEDGMENTS

The authors would like to thank Qi(Peter) Li, Uday Jain, and Josh Hajicek from Li Creative Technology, Inc. for discussing the specifications of the robots, and Karen Coyne and Daniel Barker from U.S. Army Edgewood Chemical Biological Center for providing the motivations for this project.

REFERENCES

[1] Augustus A. White, Manohar M. Panjabi. Clinical Biomechanics of the Spine, 2nd ed. *Philadelphian: JB Lippincott*, pp. 85-125, 1990.
[2] L. Gepper. Qrio, The Robot that Could, *IEEE Spectrum*, 41(5): 34-37, 2004.
[3] Y. Sakagami, R. Watanabe, C. Aoyama, S. Matsunaga, N. Higaki, K. Fujimura. The Intelligent ASIMO: System Overview and Integration. *in IEEE/RSJ International Conference on Intelligent Robots and System*, Lausanne, Switzerland, vol. 3, pp. 2478-2483, 2002.
[4] H. Ishigruo. Scientific Issures Concerning Androids. *The International Journal of Robotics Research* 26(1): 105-117, 2007.
[5] R. Beira, M. Lopes, M. Praca, et.al. Design of the Robot-Cub (iCub) Head. *in IEEE International Conference on Robotics and Automation*, Orlando, USA, pp. 94-100, 2006.
[6] H. Hirukawa, F. Kanehiroa, K. Kanekoa, etc. Humanoid Robotics Platforms Developed in HRP. *Robotics and Autonomous Systems*, 48: 165-175, 2004.
[7] Ill-Woo Park, Jung-Yup Kim, Baek-Kyu Cho, Jun-Ho Oh. Control Hardware Integration of a Biped Humanoid Robot with an Android Head. *Robotics and Autonomous Systems*, 56: 95-103, 2008.
[8] J.D. Han, S.Q. Zeng, K.Y. Tham, M. Badgero and J.Y. Weng. Dav: A Humanoid Robot Platform for Autonomous Mental Development. *in Proceedings of the 2nd International Conference on Development and Learning*, Cambridge, USA, pp.73-81, 2002.
[9] H. Miwa, T. Okuchi, H. Takanobu, A. Takanishi. Development of a New Human-like Head Robot WE-4. *in Proceedings of the 2002 IEEE/RSJ Intl. Conference on Intelligent Robots and Systems*, EPFL, Lausanne, Switzerland, vol. 3, pp. 2443-2448, 2002.
[10] A. Albers, S. Brudniok, J. Ottnad, C. Sauter, K. Sedchaicham. Upper Body of a New Humanoid Robot-the Design of ARMAR III. *in IEEE-RAS International Conference on Humanoid Robots*, Genova, Italy, pp. 308-313, 2006.
[11] G. Carbone, Hun-ok Lim, A. Takanishi, M. Ceccarelli. Stiffness Analysis of Biped Humanoid Robot WABIAN-RIV. *Mechanism and Machine Theory*, 41: 17-40, 2006.
[12] J. Hirth, N. Schmitz, K. Berns. Emotional Architecture for the Humanoid Robot Head ROMAN. *in IEEE International Conference on Robotics and Automation*, Roma, Italy, pp. 2150-2155, 2007.
[13] J. M.Sabater, N. Garcia, C. Perez, J.M. AzorinR, J. Saltaren and E. Yime. Design and Analysis of a Spherical Humanoid Neck Using Screw Theory. *in The First IEEE/RAS-EMBS International Conference on Biomedical Robotics and Biomechatronics*, pp. 1166-1171, 2006.
[14] Wowwee. Wowwee Alive Elvis. http:// www. wowweealiveonline. com/elvis/index. html, 2008.
[15] T. Hashimoto, S. Hitramatsu, T. Tsuji and H. Kobayashi. Development of the Face Robot SAYA for Rich Facial Expressions. *in SICE-ICASE International Joint Conference*, Busan, Korea, pp. 5423-5428, 2006.
[16] W. H. Wittrick. On Elastic Wave Propagation in Helical Spring. *International Journal of Mechanical Sciences*, 8: 25-47, 1966.
[17] S. Timoshenko. Theory of Elastic Stability. *New York: McGraw-Hill*, 1936.
[18] A. M. Wahl. Mechanical Springs. *New York: McGraw-Hill*, 1963.
[19] R. Frisch-Fay. Flexible Bars. *Washington: Butter Worths*, 1962.
[20] S. Timoshenko, D. H. Young. Advanced Dynamics. *New York: McGraw-Hill*, 1948.
[21] Andrew C. Sterling, Daniel G. Cobian, Paul A. Anderson, etc. Annual Frequency and Magnitude of Neck Motion in Healthy Individuals. *Spine*, 33(17): 1882-1888, 2008.